Black Hole Close Hyperbolic Encounters: Part I

Gonzalo Morrás

Instituto de Física Teórica UAM/CSIC, Universidad Autónoma de Madrid, Cantoblanco
28049 Madrid, Spain

Oct 11, 2022

Introduction

- Keplerian 2-body problem:
  - Trajectory can be described by an ellipse (e<1), parabola (e=1) or hyperbola (e>1)
- In GR, the BH 2-body problem is modified by energy loss due to GW emission
  - Elliptic trajectories ($e_0 < 1$) now circularize and eventually merge
  - Hyperbolic trajectories now have two options:
    - Energy loss is sufficiently large to bind both BHs: **dynamical capture**
    - Kinetic energy overcomes energy loss and BHs just scatter: **hyperbolic encounter**
  - If hyperbolic encounters are close enough (CHEs), energy emission can be very significant. Source of GWs!

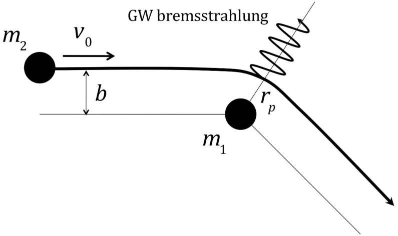

Figure 1: Schematic representation of a Hyperbolic Encounter. Credit: García-Bellido et al 2018.

Motivation I

- Evidence that black holes are in dynamical environments might already be present in the data
  - Evidence for dynamical binary assemble with $\chi_{\text{eff}} < 0$
- Some models predict dense black hole clusters in our universe
  - Models for the centers of active galactic nuclei (AGNs) and globular clusters (see Mark Gieles talk)
  - Primordial black hole models
- Black holes in these dense clusters scatter off each other in hyperbolic orbits and emit GWs.

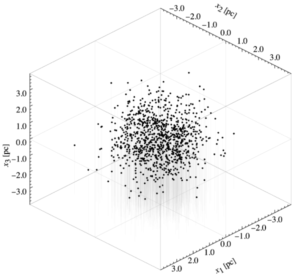

Figure 2: Initial positions for a simulated cluster of Black Holes. Credit: Trashorras et al 2022.

Motivation II

- Black Hole Hyperbolic encounters can have multiple phenomenological implications:
  - The GWs emitted can be directly detected as a burst-like signal in ground based and space interferometers (see Morrás et al 2021)
  - The GWs generate a stochastic GW background (see Jaraba et al 2022).
  - They will dissipate energy in the cluster
  - The BHs can acquire significant spin during the encounter (see Jaraba et al 2021)

Modeling

- Problem: Scattering of two gravitationally interacting masses m_1 and m_2 with spins $\vec{\mathcal{S}}_1$ and $\vec{\mathcal{S}}_2$
- No analytical solution in General Relativity (GR)
- Two ways to approach the problem
  - Numerical Relativity. Very accurate but computationally expensive (see Santiago's talk)
  - Approximate the problem using Effective One Body (EOB) and Post-Newtonian (PN) aproximations (e.g. `TEOBNResumS` spoken about in the taks of Simone, Rossella and Alessandro or Morras et al 2021)

Post Newtonian waveforms

- The Post Newtonian (PN) approximation is an expansion of GR in powers of $1/c^2$.
- To characterize CHEs it makes sense to use the Post Newtonian (PN) approximation because:
  - Simplest possible approach.
  - BHs do not get as close as in CBC (there is no merger).
  - Accurately following the phase for many cycles is not as critical.
- To capture main phenomenology we take up to leading order spin effects $\rightarrow O(1/c^3) \rightarrow 1.5$PN

Hamiltonian Formulation of the problem

- Hamiltonian of the system:

$$H(\vec{r}, \vec{p}, \vec{S}_1, \vec{S}_2) = H_{\rm N}(\vec{r}, \vec{p}) + H_{\rm 1PN}(\vec{r}, \vec{p}) + H_{\rm SO}(\vec{r}, \vec{p}, \vec{S}_1, \vec{S}_2) + O\left(\frac{1}{c^4}\right) ,$$

where

$$H_{\rm N}(\vec{r}, \vec{p}) = \frac{p^2}{2} - \frac{1}{r} ,$$

$$H_{\rm 1PN}(\vec{r}, \vec{p}) = \frac{1}{c^2}\left(\frac{1}{8}(3\eta - 1)(p^2)^2 - \frac{1}{2}\left[(3+\eta)p^2 + \eta(\hat{n}\cdot\vec{p})^2\right]\frac{1}{r} + \frac{1}{2r^2}\right) ,$$

$$H_{\rm SO}(\vec{r}, \vec{p}, \vec{S}_1, \vec{S}_2) = \frac{1}{c^2 r^3}(\vec{r}\times\vec{p})\cdot\vec{S}_{\rm eff} , \quad \text{where: } \vec{S}_{\rm eff} = \delta_1\vec{S}_1 + \delta_2\vec{S}_2 .$$

- To get the equations of motion we use Poisson's brackets:

$$\{r_i, p_j\} = \delta_{ij} ,$$
$$\{S_{1i}, S_{1j}\} = \epsilon_{ijk} S_{1k} ,$$
$$\{S_{2i}, S_{2j}\} = \epsilon_{ijk} S_{2k} .$$

Constants of motion

- From the equations of motion: $|\vec{L}|$, $|\vec{S}_1|$, $|\vec{S}_2|$, $\vec{L}\cdot\vec{S}_{\text{eff}}$ and $\vec{J}=\vec{L}+\vec{S}_1+\vec{S}_2$ are conserved.
- Note that $\hat{L}$, $\hat{S}_1$ and $\hat{S}_2$ are in general not conserved and the system precesses.
- With this Hamiltonian, the energy $E=H$ would be conserved ($\partial_t H = 0$), but we add radiation reaction effects, since they can give important phenomenology.
- The system doesn't have enough constants of motion to be integrable $\rightarrow$ numerical integration is necessary.
- We do some manipulations to maximally simplify the equations that have to be integrated.

Differential equations

$$\frac{d\bar{\xi}}{dt} = -\,c^3\frac{\bar{\xi}^{11/3}8\eta}{5\beta^7}\left[-49\beta^2-32\beta^3+35(e_t^2-1)\beta-6\beta^4+9e_t^2\beta^2\right], \leftarrow \text{Mean Motion}$$

$$\frac{de_t}{dt} = -\,c^3\frac{\bar{\xi}^{8/3}8\eta(e_t^2-1)}{15\beta^7 e_t}\left[-49\beta^2-17\beta^3+35(e_t^2-1)\beta-3\beta^4+9e_t^2\beta^2\right], \leftarrow \text{Eccentricity}$$

$$\begin{aligned}\frac{d\Phi}{dt} =& \frac{c^3\bar{\xi}\sqrt{e_t^2-1}}{(e_t\cosh v-1)^2}\left[1-\bar{\xi}^{2/3}\left(\frac{\eta-4}{e_t\cosh v-1}-\frac{\eta-1}{e_t^2-1}\right)\right.\\ &\left.-\,\bar{\xi}\frac{\Sigma}{\sqrt{e_t^2-1}}\left(\frac{1}{e_t\cosh v-1}+\frac{1}{e_t^2-1}\right)\right]-\dot{\alpha}\cos\iota\,, \leftarrow \text{Phase}\end{aligned}$$

$$\frac{d\hat{s}_1}{dt} =\delta_1\frac{c^3\bar{\xi}^{5/3}\sqrt{e_t^2-1}}{(e_t\cosh v-1)^3}\hat{k}\times\hat{s}_1\,, \leftarrow \text{Primary Spin Direction}$$

$$\frac{d\hat{s}_2}{dt} =\delta_2\frac{c^3\bar{\xi}^{5/3}\sqrt{e_t^2-1}}{(e_t\cosh v-1)^3}\hat{k}\times\hat{s}_2\,, \leftarrow \text{Secondary Spin Direction}$$

$$\frac{d\hat{k}}{dt} =\frac{c^4\bar{\xi}^2}{(e_t\cosh v-1)^3}(\delta_1S_1\hat{s}_1+\delta_2S_2\hat{s}_2)\times\hat{k}\,. \leftarrow \text{Orbital Angular Momentum Direction}$$

Solution to differential equations

- We have 11 independent variables that have to be integrated.
- The relation between t and v is obtained by solving Kepler's equation ($c^3\bar{\xi}t = e_t \sinh v - v$). This is done very efficiently with Mikkola's method.
- The differential equations are very well behaved and can be rapidly solved with standard methods such as Runge-Kutta.
- The whole process of integrating the equations of motion and computing the GWs takes $\sim$ 1s for typical LIGO-Virgo waveforms.

Solution for the orbit

- The orbit will depend on:
  - Black hole masses m_1, m_2
  - Black hole initial spins $\vec{S}_1$, $\vec{S}_2$
  - Initial eccentricity e_{t0}
  - Impact parameter b
  - Initial orbital azimutal angle Φ_0
  - Orbital inclination angle Θ

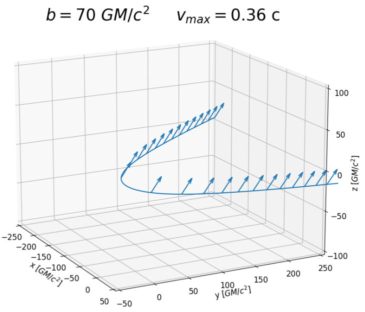

Figure 3: Example of an orbit for maximally spinning black holes with $m_1 = 20M_\odot$, $m_2 = 15M_\odot$, $b = 70Gm/c^2$, $e_{t0} = 1.1$, $\Phi_0 = 0$, $\theta_1^i = 0.5$ rad, $\phi_1^i = 0.35$ rad, $\theta_2^i = 0.8$ rad, $\phi_2^i = 1$ rad. The arrow represents $\vec{S}_{\rm eff}$.

GWs derived from the orbit

- GWs can computed from the orbit.
- Use formula with up to leading order spin effects:

$$
\begin{aligned}
h_\times = 4\frac{Gm\eta}{c^4R'}\Bigl\{&[-(\boldsymbol{p}\cdot\boldsymbol{n})(\boldsymbol{q}\cdot\boldsymbol{n})z+(\boldsymbol{p}\cdot\boldsymbol{v})(\boldsymbol{q}\cdot\boldsymbol{v})]-\frac{\delta}{c}[(\{[3(\boldsymbol{N}\cdot\boldsymbol{n})\dot r-(\boldsymbol{N}\cdot\boldsymbol{v})](\boldsymbol{q}\cdot\boldsymbol{n})-3(\boldsymbol{N}\cdot\boldsymbol{n})(\boldsymbol{q}\cdot\boldsymbol{v})\}(\boldsymbol{p}\cdot\boldsymbol{n})-3(\boldsymbol{N}\cdot\boldsymbol{n})(\boldsymbol{q}\cdot\boldsymbol{n})(\boldsymbol{p}\cdot\boldsymbol{v}))z\\
&+2(\boldsymbol{p}\cdot\boldsymbol{v})(\boldsymbol{q}\cdot\boldsymbol{v})(\boldsymbol{N}\cdot\boldsymbol{v})]+\frac{1}{6c^2}[6(1-3\eta)(\boldsymbol{N}\cdot\boldsymbol{v})^2(\boldsymbol{p}\cdot\boldsymbol{v})(\boldsymbol{q}\cdot\boldsymbol{v})+([(6\eta-2)(\boldsymbol{N}\cdot\boldsymbol{v})^2(\boldsymbol{q}\cdot\boldsymbol{n})+(48\eta-16)(\boldsymbol{N}\cdot\boldsymbol{v})(\boldsymbol{N}\cdot\boldsymbol{n})(\boldsymbol{q}\cdot\boldsymbol{v})]\\
&\times(\boldsymbol{p}\cdot\boldsymbol{n})+(48\eta-16)(\boldsymbol{N}\cdot\boldsymbol{v})(\boldsymbol{N}\cdot\boldsymbol{n})(\boldsymbol{p}\cdot\boldsymbol{v})(\boldsymbol{q}\cdot\boldsymbol{n})+((-14+42\eta)(\boldsymbol{N}\cdot\boldsymbol{n})^2-4+6\eta)(\boldsymbol{q}\cdot\boldsymbol{v})(\boldsymbol{p}\cdot\boldsymbol{v}))z+(-9\eta+3)(\boldsymbol{q}\cdot\boldsymbol{v})\\
&\times(\boldsymbol{p}\cdot\boldsymbol{v})v^2+(29+(7-21\eta)(\boldsymbol{N}\cdot\boldsymbol{n})^2)(\boldsymbol{q}\cdot\boldsymbol{n})(\boldsymbol{p}\cdot\boldsymbol{n})z^2+((-9\eta+3)(\boldsymbol{N}\cdot\boldsymbol{n})^2-10-3\eta)(\boldsymbol{q}\cdot\boldsymbol{n})(\boldsymbol{p}\cdot\boldsymbol{n})zv^2+([(-36\eta+12)\\
&\times(\boldsymbol{N}\cdot\boldsymbol{v})(\boldsymbol{N}\cdot\boldsymbol{n})(\boldsymbol{q}\cdot\boldsymbol{n})+((15-45\eta)(\boldsymbol{N}\cdot\boldsymbol{n})^2+10+6\eta)(\boldsymbol{q}\cdot\boldsymbol{v})](\boldsymbol{p}\cdot\boldsymbol{n})+[(15-45\eta)(\boldsymbol{N}\cdot\boldsymbol{n})^2+10+6\eta](\boldsymbol{p}\cdot\boldsymbol{v})(\boldsymbol{q}\cdot\boldsymbol{n}))\dot r z\\
&+((45\eta-15)(\boldsymbol{N}\cdot\boldsymbol{n})^2-9\eta+3)(\boldsymbol{q}\cdot\boldsymbol{n})(\boldsymbol{p}\cdot\boldsymbol{n})\dot r^2 z]+\frac{z^2(\boldsymbol{q}\cdot\boldsymbol{n})}{c^2}[X_2\chi_2(\boldsymbol{p}\cdot(\boldsymbol{s}_2\times\boldsymbol{N}))-X_1\chi_1(\boldsymbol{p}\cdot(\boldsymbol{s}_1\times\boldsymbol{N}))]\Bigr\},\\
h_+ = 2\frac{Gm\eta}{c^4R'}\Bigl\{&[((\boldsymbol{q}\cdot\boldsymbol{n})^2-(\boldsymbol{p}\cdot\boldsymbol{n})^2)z+(\boldsymbol{p}\cdot\boldsymbol{v})^2-(\boldsymbol{q}\cdot\boldsymbol{v})^2]-\frac{\delta}{2c}[((\boldsymbol{N}\cdot\boldsymbol{n})\dot r-(\boldsymbol{N}\cdot\boldsymbol{v}))z(\boldsymbol{p}\cdot\boldsymbol{n})^2-6z(\boldsymbol{N}\cdot\boldsymbol{n})(\boldsymbol{p}\cdot\boldsymbol{n})(\boldsymbol{p}\cdot\boldsymbol{v})+(-3(\boldsymbol{N}\cdot\boldsymbol{n})\dot r\\
&+(\boldsymbol{N}\cdot\boldsymbol{v}))z(\boldsymbol{q}\cdot\boldsymbol{n})^2+6z(\boldsymbol{N}\cdot\boldsymbol{n})(\boldsymbol{q}\cdot\boldsymbol{n})(\boldsymbol{q}\cdot\boldsymbol{v})+2((\boldsymbol{p}\cdot\boldsymbol{v})^2-(\boldsymbol{q}\cdot\boldsymbol{v})^2)(\boldsymbol{N}\cdot\boldsymbol{v})]+\frac{1}{6c^2}[6(\boldsymbol{N}\cdot\boldsymbol{v})^2((\boldsymbol{p}\cdot\boldsymbol{v})^2-(\boldsymbol{q}\cdot\boldsymbol{v})^2)(1-3\eta)\\
&+([6\eta-2](\boldsymbol{N}\cdot\boldsymbol{v})^2(\boldsymbol{p}\cdot\boldsymbol{n})^2+(96\eta-32)(\boldsymbol{N}\cdot\boldsymbol{v})(\boldsymbol{N}\cdot\boldsymbol{n})(\boldsymbol{p}\cdot\boldsymbol{v})(\boldsymbol{p}\cdot\boldsymbol{n})+(-6\eta+2)(\boldsymbol{N}\cdot\boldsymbol{v})^2(\boldsymbol{q}\cdot\boldsymbol{n})^2+(-96\eta+32)(\boldsymbol{N}\cdot\boldsymbol{v})\\
&\times(\boldsymbol{N}\cdot\boldsymbol{n})(\boldsymbol{q}\cdot\boldsymbol{v})(\boldsymbol{q}\cdot\boldsymbol{n})+[(-14+42\eta)(\boldsymbol{N}\cdot\boldsymbol{n})^2-4+6\eta](\boldsymbol{p}\cdot\boldsymbol{v})^2+[(-42\eta+14)(\boldsymbol{N}\cdot\boldsymbol{n})^2+4-6\eta](\boldsymbol{q}\cdot\boldsymbol{v})^2)z\\
&+((-9\eta+3)(\boldsymbol{p}\cdot\boldsymbol{v})^2+(-3+9\eta)(\boldsymbol{q}\cdot\boldsymbol{v})^2)v^2+([29+(7-21\eta)(\boldsymbol{N}\cdot\boldsymbol{n})^2](\boldsymbol{p}\cdot\boldsymbol{n})^2+[-29+(21\eta-7)(\boldsymbol{N}\cdot\boldsymbol{n})^2](\boldsymbol{q}\cdot\boldsymbol{n})^2)z^2\\
&+(((-9\eta+3)(\boldsymbol{N}\cdot\boldsymbol{n})^2-10-3\eta)(\boldsymbol{p}\cdot\boldsymbol{n})^2+((-3+9\eta)(\boldsymbol{N}\cdot\boldsymbol{n})^2+10+3\eta)(\boldsymbol{q}\cdot\boldsymbol{n})^2)zv^2+((-36\eta+12)(\boldsymbol{N}\cdot\boldsymbol{v})(\boldsymbol{N}\cdot\boldsymbol{n})\\
&\times(\boldsymbol{p}\cdot\boldsymbol{n})^2+((-90\eta+30)(\boldsymbol{N}\cdot\boldsymbol{n})^2+20+12\eta)(\boldsymbol{p}\cdot\boldsymbol{v})(\boldsymbol{p}\cdot\boldsymbol{n})+(-12+36\eta)(\boldsymbol{N}\cdot\boldsymbol{v})(\boldsymbol{N}\cdot\boldsymbol{n})(\boldsymbol{q}\cdot\boldsymbol{n})^2+((90\eta-30)(\boldsymbol{N}\cdot\boldsymbol{n})^2\\
&-12\eta-20)(\boldsymbol{q}\cdot\boldsymbol{v})(\boldsymbol{q}\cdot\boldsymbol{n}))z\dot r+([(45\eta-15)(\boldsymbol{N}\cdot\boldsymbol{n})^2-9\eta+3](\boldsymbol{p}\cdot\boldsymbol{n})^2+((15-45\eta)(\boldsymbol{N}\cdot\boldsymbol{n})^2-3+9\eta)(\boldsymbol{q}\cdot\boldsymbol{n})^2)z\dot r^2]\\
&+\frac{z^2}{c^2}[(\boldsymbol{p}\cdot\boldsymbol{n})(X_2\chi_2[\boldsymbol{p}\cdot(\boldsymbol{s}_2\times\boldsymbol{N})]-X_1\chi_1[\boldsymbol{p}\cdot(\boldsymbol{s}_1\times\boldsymbol{N})])+(\boldsymbol{q}\cdot\boldsymbol{n})(X_1\chi_1[\boldsymbol{q}\cdot(\boldsymbol{s}_1\times\boldsymbol{N})]-X_2\chi_2[\boldsymbol{q}\cdot(\boldsymbol{s}_2\times\boldsymbol{N})])\Bigr\}
\end{aligned}
$$

GWs derived from the orbit

- Substituting the orbit of the example of Fig. 3, we obtain:

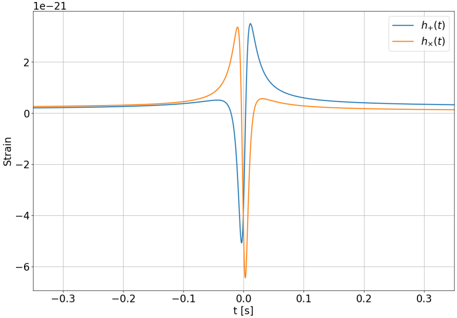

Figure 4: Gravitational waves emitted by the system shown in Fig. 3 assuming it happens at a distance $R = 20$Mpc and with an inclination of the orbit $\Theta = 45^\circ$. $t = 0$ represents the time of closest approach.

- Quadrupolar nature of the GWs $\rightarrow f_{\mathrm{GW}} = 2 f_{\mathrm{orbit}}$
- CHE perform “half” of an orbit $\rightarrow$ GWs from CHE perform one oscillation.

Example of projected GWs

- Detectors measure $h \equiv \frac{\delta L}{L} = F_+(\theta, \phi, \psi)h_+ + F_\times(\theta, \phi, \psi)h_\times \equiv h$.
- CHEs look like a common transient source of noise called blip glitch.
- The difference with glitches is that GWs are seen simultaneously in all detectors

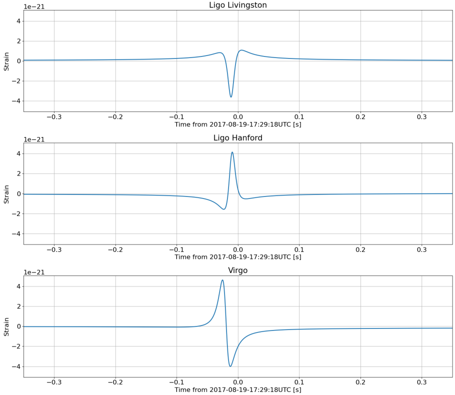

Figure 5: Result of projecting the GWs of Fig. 4 into the GW detectors, assuming that they come from $\delta = 1.0$rad, $\alpha = 3.7$rad, with $\psi = 0.2$rad and arrive at Earth at 17:29:18UTC of 2017-08-19.

CHEs in the frequency domain

- CHEs are typically low frequency signals, with a characteristic frequency $f_c \sim \frac{2}{\Delta t} \sim \frac{2v_c}{d_c} \sim 20\mathrm{Hz}\left(\frac{v_c}{0.1c}\right)\left(\frac{1000R_{S\odot}}{d_c}\right)$,
- Δt is the duration of the encounter and v_c and d_c are the characteristic speeds and distances.

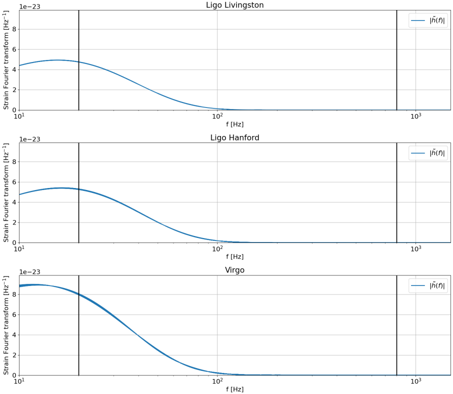

Figure 6: Fourier transform of the GW in Fig. 5. Black lines at 20 and 800Hz show the LIGO band.

CHEs in real detector data

- Inject example CHE in the detector data: $s(t) = s_{exp}(t) + h_{CHE}(t)$
- Represent it in the time-frequency domain with the Q transform.

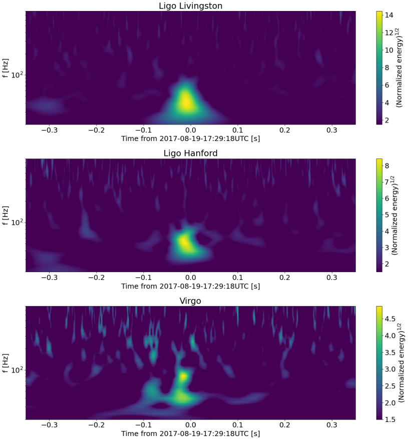

Figure 7: Square root of the normalized energy obtained by Q transforming the example CHE injected in the detector data. The signal has an optimum SNR of 20.1 in Livingston, 11.1 in Hanford and 6.7 in Virgo, for a total SNR of 23.9

CHEs in real detector data

- CHEs are best searched with burst pipelines
  - Since the GWs have only one orbit, matched-filtering presents little advantage
  - The main source of noise comes from blip glitches
  - Ability to reject these glitches is most important
- The LVK colaboration does unmodelled short-duration searches (Abbott et al. 2021) and have found no CHE candidates
- Independent more targeted searches using machine learning (see Morras et al 2021) have found no confident CHE candidates either

Conclusions

- Hyperbolic encounters are an interesting source of GWs to study.
- They can be produced in dynamical and dense black hole environments.
- They can be modeled using PN approximations of General Relativity.
- The signal is typically low frequency and morphologically very similar to a blip glitch.